Laser remanufacturing based on the integration of reverse engineering and laser cladding

Liangliang Nan*, Weijun Liu and Kai Zhang

Laboratory of Advanced Manufacturing Technology,
Shenyang Institute of Automation,
Chinese Academy of Sciences,
No. 114, Nanta Street, Shenyang,
Liaoning Province, 110016, China
E-mail: liangliang.nan@gmail.com
E-mail: wjliu@sia.cn
E-mail: kzhang@sia.cn
*Corresponding author

Abstract: Laser remanufacturing has been used as an approach to refurbish or to improve the surface quality of high-priced parts. However, most of the existing systems lack measuring and modelling functions, which results in the uncertainty of the quality of end products. This paper presents a three-dimensional Laser Remanufacturing System (LRS) based on the integration of reverse engineering and laser cladding. A coaxial powder feeding system is developed to meet the requirement of three-dimensional laser cladding. Meanwhile, the geometric and mechanical properties of metal parts of layers fabricated by LRS are explored. In addition, the principle, advantages and applications of the LRS system are described.

Keywords: laser remanufacturing; reverse engineering; laser cladding; repair technology; CAD/CAM.

Reference to this paper should be made as follows: Nan, L.L., Liu, W.J. and Zhang, K. (2011) 'Laser remanufacturing based on the integration of reverse engineering and laser cladding', *Int. J. Computer Applications in Technology*, Vol. 40, No. 4, pp.254–262.

Biographical notes: L.L. Nan is a Doctoral Student of the Graduate School of Chinese Academy of Sciences. He majors in Mechatronics Engineering in Shenyang Institute of Automaton, Chinese Academy of Sciences. He received his Bachelor's Degree in Material Science from Nanjing University of Aeronautics and Astronautics, and Master's Degree in Mechatronics Engineering from Shenyang Institute of Automation, Chinese Academy of Sciences. His research interests include reverse engineering, laser remanufacturing and CAD/CAM.

W.J. Liu is a Full Professor of Shenyang Institute of Automation, Chinese Academy of Sciences. He earned his Bachelor's Degree and Master's Degree in Mechanical Engineering from Shenyang University of Technology, and PhD in Mechanical Manufacturing from Dalian University of Technology. He is now the Director of the Rapid Prototyping Laboratory in Shenyang Institute of Automation. His current research interests include rapid prototyping, reverse engineering and rapid tooling.

K. Zhang is a Doctoral Student of the Graduate School of Chinese Academy of Sciences. He received both his Bachelor's Degree and Master's Degree in Material Science from Northeast University. His research interests include laser cladding and rapid prototyping.

1 Introduction

In machine shops and tool factories all over the world, repair personnel struggle to stretch the lifespan of vital pieces of equipment. Conventional techniques such as electroplating, repair welding and spraying (thermal and plasma) have various limitations. Because electroplated layers are too thin, this process cannot be used to repair parts with shape defects. Sometimes welding can extend the life of damaged components in aircraft, tanks and other industrial machines. But, in some cases, high-temperature welding processes do more harm than good, warping and weakening delicate metal components because of the large amount of heat involved. Welding induces excessive heat and a large Heat Affected Zone (HAZ), which may destroy the usefulness of the part. Previously, such components would be classified as irreparable and have to be replaced with pricey new parts (Grylis, 2003). So, developing a reliable repair technology to extend the life of aging pivotal parts with wide applicability and high accuracy is an urgent task.

Over the last three decades, with the development of laser cladding and its application in rapid prototyping, especially in direct metal fabrication, this new process can be used as a means to repair metal parts (Griffith et al., 1996; Link et al., 1998). Laser cladding has been defined as a process that is used to fuse with a laser beam another material that has different metallurgical properties on a substrate. The equipment for laser cladding consists mainly of four parts: a carbon dioxide laser as heat source, a powder delivery system, a working table and a Computerised Numerical Control (CNC) controller.

Laser cladding is based on a simple principle. During the cladding process, the laser beam focuses on the surface of the metal part and forms a molten pool. Meanwhile, additive materials (always metal powders) carried by gravity or gas are delivered into the molten pool. The workpiece moves under the control of a computer, and the focused laser beam moves away, the molten pool solidifies and the additive material fuses with the substrate. Thus, the laser beam scans line by line, layer by layer, and finally produces a three-dimensional shape.

To refurbish a metal part, the Computer-Aided Design (CAD) model of the part is required for tool path planning. However, the CAD model of the part is not always available, which becomes one of the main obstacles to implementing the LRS. Fortunately, the integration of laser cladding and reverse engineering makes this task feasible.

This paper is organised as follows. Section 1 is the current introduction. Section 2 is devoted to present the implementation of the recommended LRS. Section 3 gives some experimental results of the geometric and mechanical properties of metal parts and layers fabricated by the LRS machine. Applications of laser remanufacturing and its advantages are presented in Section 4. Finally, concluding remarks are given in Section 5.

2 Implementation of the recommended LRS

To get the machining path, the CAD model is needed. In this research, reverse engineering is integrated with laser cladding to construct the CAD model, and then to generate the machining path. Two types of machining path generation approaches are described.

2.1 Reverse engineering

In the process of part or product design, reverse engineering is an important method for constructing a CAD model from a physical part that already exists (Milroy et al., 1995; Fitzgibbon et al., 1997; Várady et al., 1997; Ma and Kruth, 1998). Most of the proposed solutions for reverse engineering are realised by two steps: digitising and surface modelling (Figure 1). During the first step, the metal part to be repaired is measured or digitised by a measuring device (three-dimensional digitiser), for example, a Coordinate Measuring Machine (CMM) or a laser scanner and the surface points of the part are captured in three-dimensional coordinates. Depending on the measuring hardware used and measuring strategies applied, the measured points can be distributed in sectional lines (regular or irregular), or even randomly. During the second step, a CAD model is reconstructed from the measured points.

Figure 1 Two-step reverse engineering approach

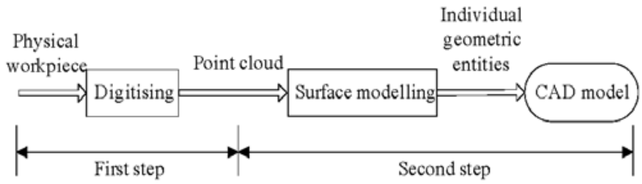

2.1.1 The acquisition of point cloud data

The digitising of a three-dimensional shape is an actual research and development field that is related to the problem of processing images acquired from accurate optical triangulation. The range data acquired by a three-dimensional digitiser (for example an optical triangulation scanner) commonly consists of depths sampled on a regular grid, which is a sample set known as a range image. A number of techniques have been developed for reconstructing surfaces by integrating groups of aligned range images.

Laser three-dimensional digitisers bring more automation to data gathering. These devices scan without contacting the profile of a physical model by a striped laser beam and CCD cameras capture profile images from which digital data (point cloud data) can be generated by triangulation algorithms. Using this method, hundreds of surface points can be obtained per second. It will take only a few minutes to digitise the worn metal part, no matter how complex its surface geometry is. In this research, a three-dimensional digitiser based on stereo-view has been established by Shenyang Institute of Automation, Chinese Academy of Sciences. Figure 2 shows the illustration of the data acquiring system.

Figure 2 The illustration of the data acquiring system

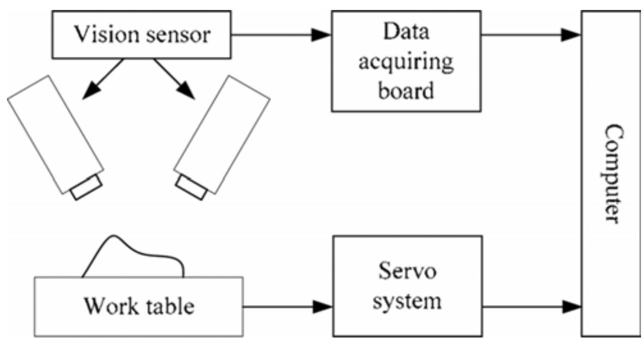

2.1.2 Surface reconstruction

For point cloud generated by a three-dimensional digitiser, two-stage modelling is needed to reconstruct the surface (Lai et al., 2001). In the first stage, a topologically triangular mesh is calculated from the point cloud; then, the NURBS surface model follows in the second stage. Before calculating the triangular mesh, data extraction is used to reduce the amount of the data points.

2.1.3 Machining path generation

Efficient machining of surfaces is very important in many manufacturing industries, such as turbine blades, shoe lasts and dies (Park, 2004). Since the quality of tool path planning affects the quality of machining to a great extent, generating an accurate machining path in an efficient manner is quite important (Sun et al., 2006). For LRS machining process, the machining path generation can be categorised into two types: generation from the reconstructed CAD model and direct generation from the point cloud.

2.1.3.1 Machining path generation from the reconstructed CAD model

Traditionally, an NC tool path is usually generated by sweeping parametric surfaces of a CAD model (Chuang et al., 2002). Many new tool path generation methods have been developed in recent years, such as principal axis method (Rao et al., 1997), uneven offset method (Shan et al., 2000), machining potential field approach (Chiou and Lee, 2002), maximum-kinematical-performance-based method (Kim and Sarma, 2002) and guide-surface-based method (Kim and Choi, 2000). These methods are very effective for the machining of free-form surfaces. For the LRS machine, the input is a two- or three-dimensional CAD model that is reconstructed from the point cloud. And, then the path generation module exports the machining path directly from the CAD model.

2.1.3.2 Direct machining path generation from the point cloud

When surfaces are machined, the most commonly used method is to approximate or fit the point cloud data sampled from the metal parts to surface data, which is the surface reconstruction process mentioned earlier. However, this process has a well-known time-consuming feature. This serves as a motivation to direct machining path generation from the digitised point cloud (Peng and Yin, 2005).

Recently, a number of papers have considered direct tool path generation from digitised point cloud data. For rough and finish machining, Lin and Liu (1998) suggested methodologies to generate a tool path from digitised point cloud data by constructing a *Z*-map model. Park and Chung (2003) and Chui et al. (2002) also presented procedures through which three-axis tool paths could be directly generated from digitised point cloud data.

Huang et al. (2006) have developed an algorithm of tool path generation from densely scattered measure points based on Constraint Quadratic Error Metrics (CQEM). We applied this algorithm to LRS machining. In this application, since there is no tool used, the focused laser beam can be assumed to be a ‘tool’. Thus, the focused point of the laser beam is the ‘cutting contact point’ (C-C point), and the nozzle head is the ‘cutting location point’ (C-L point).

2.2 Three-dimensional coaxial powder feeding subsystem

For laser cladding, the supply of the additive material is one of the key factors controlling the process. The most advantageous method is powder injection. This can be done by the use of a powder nozzle that can have several configurations. Two basic layouts are shown in Figure 3. The lateral supply of powder (also called off-axial powder injection, Figure 3(b)) allows the treatment of all kinds of shapes by applying dedicated powder nozzles. Basically, lateral powder nozzles are just tubes with the proper length, shape and diameter (Schneider, 1998). The coaxial supply of powder (Figure 3(a)) (Pelletier et al., 1994; Tucker et al., 1984; Vetter et al., 1994) can be integrated with the optical system (Schneider, 1998). An advantage of the coaxial powder supply is the independence of the powder supply from the direction in which the workpiece moves. Two other advantages of the coaxial powder supply are the controllable heating of the powder before it enters the molten pool and the high powder feed efficiency (Jouvard et al., 1997; Lemoine et al., 1994; Li et al., 1995; Vetter et al., 1994; Nan et al., 2006). Figure 4 shows the working coaxial powder nozzle of the LRS.

Figure 3 (a) Coaxial and (b) lateral powder supply

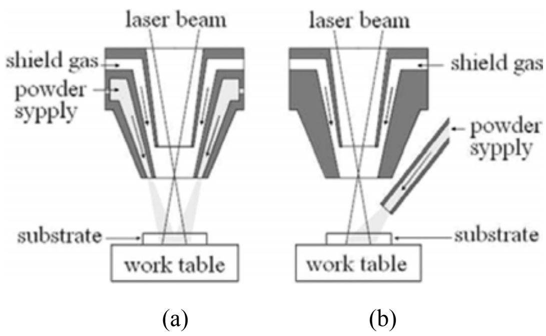

Figure 4 The working coaxial powder nozzle of the LRS

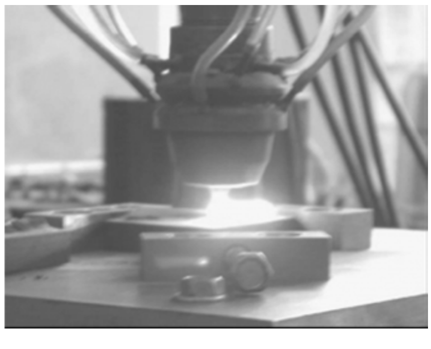

To perform three-dimensional repair, a corresponding powder feeding nozzle has been developed. In this research, a three-dimensional coaxial powder feeding subsystem is integrated in the cladding system (Figure 5).

Figure 5 The illustration of the three-dimensional coaxial powder feeding system

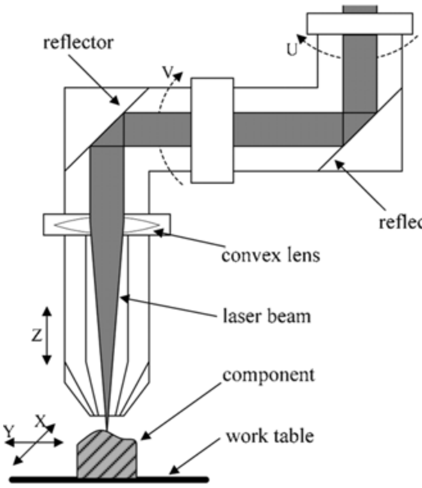

2.3 *The integration of laser cladding and reverse engineering*

The LRS is based on the integration of laser cladding and reverse engineering (Figure 6). Figure 7 shows the LRS machining developed by Shenyang Institute of Automation, Chinese Academy of Sciences.

Figure 6 The integration of reverse engineering and laser cladding

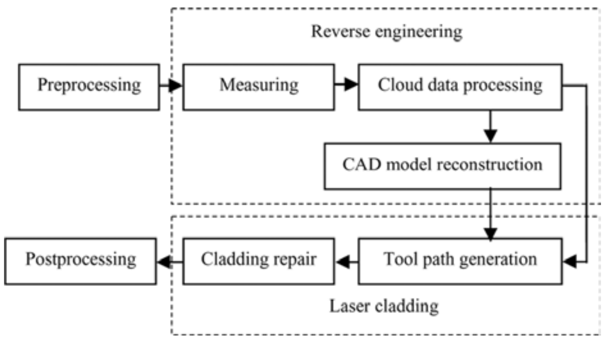

Figure 7 The LRS machine developed by Shenyang Institute of Automation, Chinese Academy of Sciences

To start the repair process, a high-powered laser beam strikes a small spot (approximately 0.5 mm wide) on the surface of the damaged metal component, producing a molten pool. Then, the powder feed nozzle delivers metal powder into the molten pool to increase its volume. This process is repeated within a plane to create a single metal layer. Then, another layer is deposited on top of that. The machine deposits layer upon layer until it has produced a metal version of the CAD model. Deposition occurs inside an argon atmosphere containing as little as one part per million of oxygen. This is crucial when working with sensitive alloys like titanium.

LRS machines feature a vision system that lets users to see the damaged part on a monitor. Crosshairs appear on top of the part image. Users can map the repair area by moving the crosshairs with a computer mouse. Then, they enter process parameters, such as the length and width of the repair. Using the map and entered data, special software generates the repair file that directs the operation of the LRS machine. Then, the system stores this information for future use. If a similar repair is needed, the operator can use the stored file rather than create a new one.

3 Geometric and mechanical properties of metal parts repaired and fabricated by LRS

3.1 *The smoothness of the forming surface*

Ideally, surfaces with high smoothness are wanted. Actually, owing to the action of surface tension of the liquid metal during the cladding process, the overlapping surface cannot be absolutely plane, which induces the convex arc shape in the cross section of one single cladding pass and the depressed area between the consecutive cladding passes. Especially, the higher the cladding layer, the bigger the curvature of the cross section, so it is critical to avoid the excessively high cladding layer.

After numbers of planar scanning experiments with different scanning spaces, the optimal overlapping rate and scanning space can be gained by measuring and comparing the cross-sectional parameters of the cladding track. With the diameter of the focused laser spot 3 mm, scanning velocity 6 mm/s, powder feed rate 4 g/min and scanning spaces orderly 2.1, 1.7 and 1.3 mm, the experimental results are shown in Figure 8. Comparing the surface results, we choose 1.3 mm as the ideal scanning space, which holds a batter profile. As can be seen from Figure 8 (right), the scanning plane is relatively smooth, the height of adjacent cladding passes is generally uniform, and the channels between the adjacent cladding tracks are comparatively shallow. Adopting such processing parameters, the smoothness of the forming surface is ensured. Sequentially, according to the bedding scanning path information obtained by the sliced CAD model, the continuous multi-layer planar scanning can be achieved successfully, which is the essence of forming whole parts.

Figure 8 Planar scanning experimental specimens with different scanning spaces. (The scanning spaces from left to right are orderly 2.1, 1.7 and 1.3 mm) (see online version for colours)

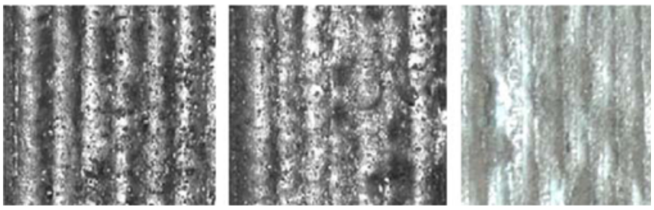

3.2 The microstructure of LRS-deposited layers

Figure 9(a) shows the SEM micrograph of the longitudinal section of the middle of the LRS-deposited layers. It shows that the solidification microstructure is composed of parallel dendrites whose growing direction is nearly parallel to positive *Z*-direction, and the dendrites take on the look of typical directional solidification microstructure in *Z*-direction. In the process of cooling solidification of the liquid metal, owing to the cooling effect caused by the substrate, heat mostly dissipates in negative *Z*-direction, so the temperature gradient in the positive *Z*-direction is remarkably dominant, which leads to the liquid metal holding the directivity. Under the action of the highest temperature gradient and solidification rate in *Z*-direction, grains grow with the directional selection, thus forming the dendrites that are almost parallel to *Z*-direction.

Figure 9(b) displays the SEM micrograph of the longitudinal section of the top of the LRS cladding layer in *Z*-direction. Apparently, equiaxed grains appear on the top of the fine dendrites. This can be explained using the metal solidification theory: the solidification microstructure essentially depends on the local solidification conditions, that is G/V_s (solidification speed V_s, temperature gradient at the solid/liquid interface G), which is the critical parameter determining the solidification microstructures. At the top of the cladding layers, the temperature gradient in the positive *Z*-direction is not dominant any more. Additionally, the heat dissipating from the surface is helpful to the metallic solidification, thus changing the distribution of the temperature gradient. As a result, G/V_s in the *Z*-direction in this region decreases substantially, thus causes that G/V_s in this region does not hold evident directivity any longer and forms the fine equiaxed grain structure.

The X-ray diffraction result of the surface of the cladding layer of a nickel-based super alloy Ni60 is demonstrated in Figure 10. It can be found that at the surface of the cladding layer, the peaks at (1, 1, 1), (2, 0, 0) and (2, 2, 0) crystal orientations are quite clear, which means that at the top of the cladding layer, the growing direction of grains is rather disorder and the solidification microstructure is not the directional solidification dendrite any longer.

Figure 9 SEM micrograph of the longitudinal section of LRS-deposited samples in *Z*-direction. (a) at the middle of the cladding layer and (b) at the top of cladding layer

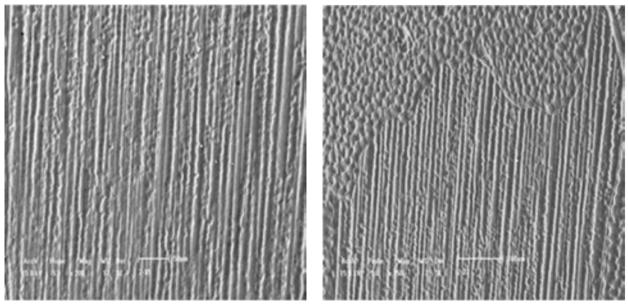

(a) (b)

Figure 10 The X-ray diffraction result of the surface of the cladding layer of a nickel-based super alloy Ni60

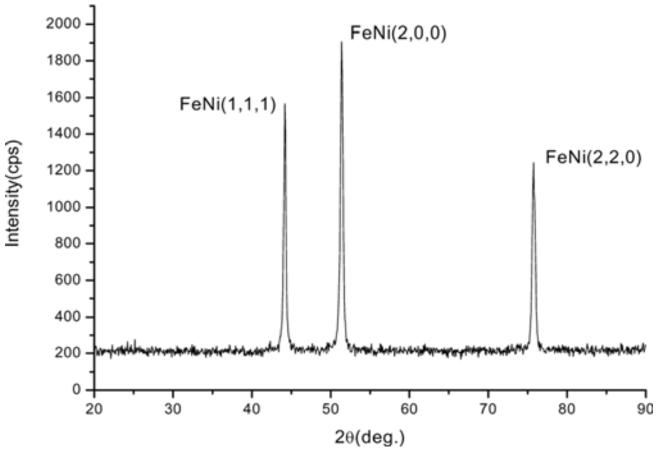

3.3 The mechanical properties of LRS-fabricated parts

With the standard tensile sample cut from an LRS-fabricated part, the normal temperature tensile experiment is performed along the scanning direction. As a result, the experimental data of ultimate strength is 430 MPa, the yield strength 355 MPa and the elongation percentage 9%. These results indicate that the tensile sample holds fine mechanical properties, meeting the requirement of properties for real usage.

Observing the SEM morphologies of fracture appearance of the tensile sample (Figure 11), a large number of dimples with various shapes and sizes that distributed in the fracture can be found. The dimples indicate that the composition phases hold rather high ductility. In other words, the parts fabricated by LRS have ductile fracture behaviours. Additionally, it can be found that plentiful round pits and white block MC phases are distributed on the dimples, also arris in the fracture. The round pits are formed by the desquamation of very hard particles. This kind of mixed fracture mechanism often occurs in the materials with high strength and fine ductility. Consequently, it can be confirmed from the fracture characteristic of LRS-formed nickel-based super alloy samples that the mechanical properties are identical to that of the conventionally fabricated parts.

Figure 11 SEM morphology of standard tensile sample

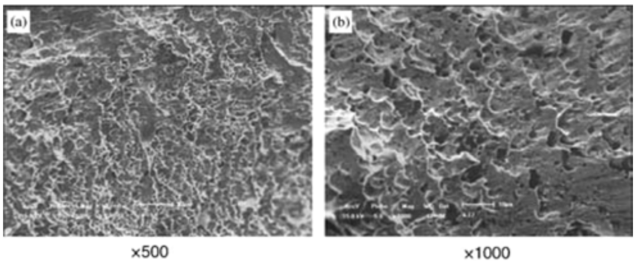

3.4 The microhardness of LRS-deposited layers

To evaluate the material property of LRS-deposited layers, the microhardness is one of the most important indices. It depends on both the composition and the microstructure of the layers. Figure 12 exhibits the distribution of the microhardness of the longitudinal section of LRS-deposited thin-wall sample in *Z*-direction. In the figure, the horizontal ordinate represents the vertical distance from the measuring point to the substrate surface of the thin-wall sample, and the vertical ordinate represents the Vickers hardness of the measuring point. It can be concluded that the hardness at the bottom and top of the thin-wall sample is higher than the hardness at the middle of the thin-wall sample.

Figure 12 The LRS-fabricated (a) thin-wall sample and its micro hardness distribution in (b) *Z*-direction

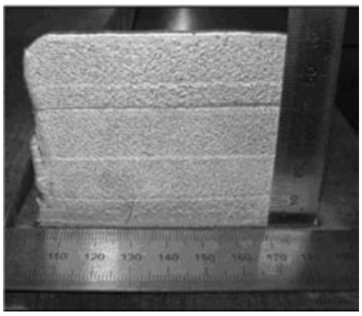

(a)

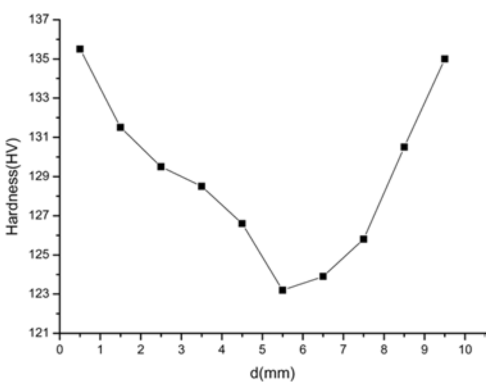

(b)

The existence of the minimum microhardness value can be explained as follows. The hardness at the top of the thin-wall sample is higher owing to the refining microstructure of the cladding layers caused by the rapid melt and solidification. However, the hardness at the middle of the thin-wall sample goes down, which is because, during every cladding cycle, namely the reciprocating motion of the laser beam, the temperature in all positions of the prior-formed sample goes through a cyclic process in which the temperature changes from low to high, then to low again, so the prior-formed positions undergo multiple heat cycles. This effect is equivalent to the disposal of multiple tempers and agings. The earlier the position formed is, the more times it undergoes the heat cycle. Therefore, the hardness of prior-formed positions, especially the middle of the sample, decreases because of this effect. But, the hardness of the bottom of the thin-wall part goes up again. The reason is that the initial several cladding layers suffer from the forced cooling function of the substrate, so the temperature gradient in this region becomes evident, forming the especially close dendrites. Summarily, the factors mentioned earlier result in the difference in the micro hardness of different positions of the LRS-fabricated thin-wall sample.

4 Applications and advantages of LRS

Laser remanufacturing technology shows extensive application in many fields, such as aerospace, planes, weapons and automobiles. It can be used to repair high-priced damaged metal parts, to improve the properties of the existing components, to fabricate functional parts and to make small lot production.

4.1 Case studies

4.1.1 Case study 1: metal part repair and quality improvement

After being used for a period, some metal parts might be eroded, worn-out, or have small surface cracks. Since laser remanufacturing is one of the specific applications of rapid prototyping, it can be used as a new repair technology for high-priced metal parts (Figure 13(a)). Some kinds of metal parts work under critical environment and thus require special mechanical properties, for example, high toughness of the main body but high wear resistance in surface. In this situation, the surface quality of the metal parts can be improved and the inner mechanical properties are kept by laser remanufacturing technique (Figure 13(b)).

4.1.2 Case study 2: direct fabrication of metal part

Other uses of laser remanufacturing technology focus on low-volume manufacture. With laser remanufacturing technology, there is no interference between tools and formed parts, so the dimension shape can be very complicated (Figure 14). Moreover, the as-deposited parts are fully dense, hold rapid solidified microstructure, and meet the requirements for direct usage. During the machining process, the substrate moves in the *X–Y* plane beneath the laser beam to deposit a thin cross-section, thereby creating the desired geometry for each layer. After deposition of each layer, the position of the powder feed nozzle and the focusing laser beam are incremented in the positive *Z*-direction (see Figure 5). As a result, successive layers are deposited to produce the entire three-dimensional component volume of fused metal representing the desired CAD model. In nature, this forming procedure is multi-layer laser cladding. This opens the door to fabricate replacement components for parts that are not repairable at the time they are needed.

Figure 13 (a) Crankshaft and (b) sleeve repaired and improved by the LRS machine

(a) (b)

Figure 14 Parts fabricated by the LRS machine (see online version for colours)

4.2 The advantages of laser remanufacturing

With the ability of one-step manufacture, this technology can greatly reduce the lead-time and investment cost of mould and die design, the fabrication of hard or rare metal components, the repair of refractory and costly components (Li et al., 2005).

4.2.1 Turning down the heat

Like common repair welding techniques, LRS can repair parts by adding metal to a heated surface. But, conventional repair welding processes can produce a large HAZ because of the large amount of heat involved, which may cause distortion or destroy the microstructure of the part. So, the integrity of a part can be compromised by the formation of a large HAZ.

LRS generates little heat, keeping the HAZ to the minimum. Because the HAZ does not spread to critical areas, LRS can fix parts once classified as irreparable because of the strength loss or distortion that would be caused by the heat from a conventional repair welding process.

4.2.2 Reducing manual tasks, resulting in faster and higher efficient repairs

The LRS machine features a computerised closed-loop control system that helps ensure precise, repeatable repair operations. During each operation, the control system monitors key variables and continually optimises the process. LRS nozzles can deposit materials in almost the exact amounts required, minimising post-process cleanup and machining. LRS also automates the process of adding material to a worn or fractured surface. Guided by the tool path data generated from the measured point cloud, LRS machines deposit metal features one layer at a time, in a fast and repeatable manner that also boosts repair quality.

After the repair process, ideal scale and geometry is obtained. Machining the excess material takes little time, compared with the excessive post-treatment after deposition to remove the large amounts of materials deposited with conventional repair welding techniques.

4.2.3 Repairing metal parts or prolonging their lives

In most cases, the tiny molten pool produced by the LRS system cools at a rate of 1000–5000° per second. Rapid material cooling and solidification produce fully dense features with greater strength and ductility than those made by other welding techniques. In some cases, the part repaired by LRS even exhibits mechanical properties that are superior to the original material. This means that the parts may stay in service longer after repair than before.

4.2.4 Lower cost of maintaining critical parts

LRS saves money by fixing parts for a fraction of the cost of manufacturing new ones. Considering a third-stage turbine rotor made of M3610C/Inconel 713LC, LRS repair costs $2000, compared with $8297 cost to fabricate a new one (Gnam et al., 2000). The NCMS (National Center for Manufacturing Sciences, USA) uses this technology to repair small, thin metal parts in the gas turbine engines of Anniston Army Depot's M1 Abrams tanks. This is projected to generate more than $6.3 million in savings annually for the DOD. Table 1 presents a direct cost comparison between laser repaired/remanufactured components with that done conventionally.

Table 1 Estimated annual cost savings (Gnam et al., 2000) (see online version for colours)

			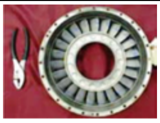
Part	*3rd stage turbine rotor*	*4th stage turbine rotor*	*2nd stage nozzle*
New part cost	\$8297	\$7168	\$6032
Estimated repair cost	\$2000	\$2000	\$2250
Saving per part	\$6297	\$5168	\$3782
Part repaired per year	230	230	600
Savings per year	\$1,448,310	\$1,188,640	\$2,269,200

5 Conclusions

Laser remanufacturing is a new repair and overhaul technology that can extend the life of aging dies, aircrafts, ships, vehicles and weapon systems. A design choice based on the integration of laser cladding and reverse engineering has been implemented.

The three-dimensional digitising methodology, gaining surface data for CAD model reconstruction, makes available fast model acquisition for machining path generation before laser remanufacturing process. To start from three-dimensional digitising of worn metal parts allows to build promptly the CAD model and thus to generate the machining path easily.

The integration of reverse engineering with laser cladding makes a faster laser repairing technology, which reduces lead-time and associated costs in mechanical industry. The usage of LRS has proven that laser remanufacturing has a wide range of application prospects.

Acknowledgements

This research is supported by the National '863' High-Technology Research Project (contract No. 2002AA420060) and the Knowledge Innovation Programs of the Chinese Academy of Sciences (grant No. F040208).

We want to thank Mike Gnam from National Center for Manufacturing Sciences (NCMS), USA and Rich Plourde from Optomec for providing us with some statistics on laser remanufactured and conventionally manufactured components. Also thanks to Dr. Paddison for assistance with the English writing and valuable suggestions in this work. Thanks to the reviewers for their valuable comments and help in improving this manuscript.

References

Chiou, C.J. and Lee, Y.S. (2002) 'A machining potential field approach to tool path generation for multi-axis sculptured surface machining', *Computer Aided Design*, Vol. 34, No. 8, pp.357–371.

Chuang, C.M., Chen, C.Y. and Yau, H.T. (2002) 'A reverse engineering approach to generating interference-free tool-paths in three-axis machine from scanned data of physical models', *International Journal of Advanced Manufacturing Technology*, Vol. 19, No. 1, pp.23–31.

Chui, K.L., Yu, K.M. and Lee, T.C. (2002) 'Direct tool-path generation from massive point input', *Proceedings of the Institute of Mechanical Engineers, Part B: Journal of Engineering Manufacture*, Vol. 216, No. 2, pp.199–206.

Fitzgibbon, A.W., Eggert, D.W. and Fisher, R.B. (1997) 'High-level CAD model acquisition from range image', *Computer-Aided Design*, Vol. 29, No. 4, pp.321–330.

Gnam, M., Plourde, R. and McDonald, T. (2000) *Laser Engineered Net Shaping (LENS)*, Retrieved 23 January, 2004 from http://www.jdmag.wpafb.af.mil/laser%20engineered%20net%20shaping.pdf

Griffith, M.L., Keicher, D.M., Atwood, C.L., Romero, J.A., Smugeresky, J.E., Harwell, L.D. and Greene, D.L. (1996) 'Free form fabrication of metallic components using laser engineered net shaping (LENS)', *Proceedings of the Solid Freeform Fabrication Symposium*, Austin, USA, pp.125–131.

Grylis, R. (2003) 'Laser system saves damaged military parts from the scrap heap', *The Fabricator*, Retrieved 3 March, 2003 from http://www.thefabricator.com/Default.cfm

Huang, Y.B., Wang, Q.F., Huang, Z.D. and Wu, J.J. (2006) 'Tool-path generation from densely scattered measure points based on CQEM', *International Journal of Advanced Manufacturing Technology*, Vol. 27, No. 9, pp.945–950.

Jouvard, J.M., Grevey, D.F. and Lemoine, F. (1997) 'Continuous wave Nd:YAG laser cladding modelling: a physical study of track creation during low power processing', *Journal of Laser Applications*, Vol. 9, No. 1, pp.43–50.

Kim, B.H. and Choi, B.K. (2000) 'Guide surface based tool path generation in three-axis milling: an extension of the guide plane method', *Computer Aided Design*, Vol. 32, No. 3, pp.191–199.

Kim, T.J. and Sarma, S.E. (2002) 'Tool path generation along directions of maximum kinematic performance; a first cut at machine-optimal paths', *Computer Aided Design*, Vol. 34, No. 6, pp.453–468.

Lai, X.M., Lin, Z.Q., Huang, T. and Zeng, Z.P. (2001) 'A study of a reverse engineering system based on vision sensor for free-form surfaces', *Computers and Industrial Engineering*, Vol. 40, No. 3, pp.215–227.

Lemoine, F., Grevey, D.F. and Vannes, A.B. (1994) 'Cross-section modelling of pulsed Nd:YAG laser cladding', *Laser Materials Processing and Machining*, *Proceedings of SPIE*, Vol. 2246, pp.37–44.

Li, P., Yang, T.P., Li, S., Liu, D.S., Hu, Q.W., Xiong, W.H. and Zeng, X.Y. (2005) 'Direct laser fabrication of nickel alloy samples', *International Journal of Machine Tools and Manufacture*, Vol. 45, No. 11, pp.1288–1294.

Li, W.B., Engström, H., Powell, J., Tan, Z. and Magnusson, C. (1995) 'Modelling of the laser cladding process – preheating of the blown powder material', *Lasers in Engineering*, Vol. 4, pp.329–341.

Lin, A.C. and Liu, H.T. (1998) 'Automatic generation of NC cutter path from massive data points', *Computer Aided Design*, Vol. 30, No. 1, pp.77–90.

Link, G.R., Fessler, J., Nickel, A. and Prinz, F. (1998) 'Rapid tooling die case inserts using shape deposition manufacturing', *Materials and Manufacturing Processes*, Vol. 13, No. 2, pp.263–274.

Ma, W. and Kruth, J.P. (1998) 'NURBS curve and surface fitting for reverse engineering', *International Journal of Advanced Manufacture Technology*, Vol. 14, No. 10, pp.918–927.

Milroy, M., Bardley, C., Vickers, G. and Weirll, J. (1995) 'A G1 continuity of B-spline surfaces batches in reverse engineering', *Computer-Aided Design*, Vol. 27, No. 6, pp.471–478.

Nan, L.L., Liu, W.J. and Zhang, K. (2006) 'Modeling for laser-material interaction to predict and control the cross sectional area of coaxial laser cladding with powder', *Proceedings of the International Conference on Advanced Design and Manufacture*, Harbin, China, pp.386–390.

Park, S.C. (2004) 'Sculptured surface machining using triangular mesh slicing', *Computer Aided Design*, Vol. 36, No. 3, pp.279–288.

Park, S.C. and Chung, Y.C. (2003) 'Tool path generation from measured data', *Computer Aided Design*, Vol. 35, No. 5, pp.467–475.

Pelletier, J.M., Sallamand, P. and Criqui, B. (1994) 'Microstructure and mechanical properties of some metal matrix composites produced on different materials by laser cladding', *Lasers in Engineering*, Vol. 3, pp.15–27.

Peng, Y.H. and Yin, Z.W. (2005) 'A new strategy for direct tool path generation from measured points', *International Journal of Production Research*, Vol. 43, No. 5, pp.933–944.

Rao, N., Ismail, F. and Bedi, S. (1997) 'Tool path planning for five-axis machining using the principal axis method', *International Journal of Machine Tools and Manufacture*, Vol. 37, No. 7, pp.1025–1040.

Schneider, M.F. (1998) *Laser Cladding with Powder: Effect of Some Machining Parameters on Clad Properties*, PhD Thesis, University of Twente, Enschede, Netherlands.

Shan, Y., Wang, S.L. and Tong, S.G. (2000) 'Uneven offset method of NC tool path generation for free-form pocket machining', *Computers in Industry*, Vol. 43, No. 1, pp.97–103.

Sun, Y.W., Guo, D.M., Jia, Z.Y. and Wang, H.X. (2006) 'Iso-parametric tool path generation from triangular meshes for free-form surface machining', *International Journal of Advanced Manufacturing Technology*, Vol. 28, Nos. 7–8, pp.721–726.

Tucker, T.R., Clauer, A.H., Wright, I.G. and Stropki, J.T. (1984) 'Laser-processed composite metal cladding for slurry erosion resistance', *Thin Solid Films*, Vol. 118, No. 11, pp.73–84.

Várady, T., Martin. R.R. and Cox, J. (1997) 'Reverse engineering of geometric models – an introduction', *Computer-Aided Design*, Vol. 29, No. 4, pp.255–268.

Vetter, P.A., Engel, T. and Fontaine, J. (1994) 'Laser cladding: the relevant parameters for process control', *Proceedings of Laser Materials Processing: Industrial and Microelectronics Applications*, Vol. 2207, pp.452–462.